Measurement of dynamic pulsations in bulk solid during silo discharging using ECT method

K. Grudzień [1], Z. Chaniecki [1], M. Niedostatkiewicz [2], A. Romanowski [1],D. Sankowski [1]

[1]Computer Engineering Department, Technical University of Łódź,Poland, kgrudzi@kis.p.lodz.pl

[2] Department of Fundamentals of Building and Material Engineering, Technical University of Gdańsk, Poland, mniedost@pg.gda.pl

Reviewer: A.J. Peyton (University of Manchester, UK)

Summary: Paper will focus on the results of tests with the slender cylindrical silo emptied both gravitationally and in controlled manner. The influence of the initial density, wall roughness, height and velocity on the emptying process will be presented. During tests values of the vertical and horizontal accelerations on the silo wall were measured, the effect of the outlet velocity and level of the dynamic effects were compared. Results will be presented in the form of continuous graphs, which allow to analyse the entire process in simpler way comparing to tomographic images form. It is a better form of presentation in order to work out settings for process control, as well.

Keywords: ECT, bulk solid concentration measurement, silo investigation, monitoring, diagnosis processes

1. Introduction

The knowledge of the bulk solid concentration during the silo flow is very important and necessary to the understand the behaviour and utilize this information in the process of silo operation, especially filling and discharging (Niedostatkiewicz and Tejchman, 2003; Chaniecki et al., 2004; Grudzień et al., 2004). Moreover, the concentration of the bulk solid has the serious influence on the operational safety of the silo structure due to possibility of the local pressure increasing on the silo wall and hopper. Accurate description of the bulk solid concentration (not only during the silo filling, but also during emptying), demands measurement methods of a non invasive character. Importance of the process diagnosis is shown in (Korbicz et al., 2002). Some methods of the description and visualisation of the bulk solid during silo flow for monitoring and diagnosis processes presented in this paper can be applied (Chaniecki, 2006; Chaniecki at al., 2006; Grudzień, 2007). Electrical Capacitance Tomography (ECT) meets this requirement and allows to monitor and diagnose process of the silo discharging by the observation of the concentration changes of the bulk solid inside the silo cross section (Chaniecki and Sankowski, 2007).

Behaviour and control of bulk solid flow phenomena in pneumatic conveying and during hopper discharge has been investigated for years, though it still remains a difficult assignment both practically and theoretically (Ostrowski et al. 1999; Neuffer et al. 1999). Wide-ranging investigation of this subject with theoretical models for powder flows analysis and interaction between air and the grains can be found in Bates (1999), Chase (2002), Dyakowski et al. (2000), Jenike (1979), and Seville et al. (1997).

Silos are a class of hoppers. Hoppers can vary in bin geometry. There are different types of hoppers varying by size, shape and material of construction. Different types of flow regimes may occur during discharging the hopper. The purpose of this paper is to show the possibilities of ECT application to exploring the dynamic behaviour of solids flow during hopper discharging. Hopper flow investigation can lead to better understanding of the nature of this process, hence resulting in eventual benefits arising from improved design of containers for storing and loading solid materials (Romanowski et al., 2006).

Hopper discharging often proceeds in the so-called funnel flow regime. Two main regions exist in hopper flow, e.g. the so-called stagnant zone (located by the walls of container) and funnel flow (usually present in the centre). These vary only in terms of a slight difference in packing density of material in the two zones. This flow results in the generation of air-filled voids. These small voids or gaps appear among the particles as they process down towards the bottom orifice. The material in the stagnant zone is expected to maintain its packing density fraction; while the material in the dynamic region is less densely packed due to the flow forced by discharging process.

2. Experimental setup

The experimental system considered here was a simplified, flat bottom model of the silo having a circular cross section. The experimental system was fabricated out of a slender cylindrical perspex (diameter D=0.2 m, height H=2.0 m, wall thickness W=0.005 m, orifice diameter d=0.07m). The material used in experiments was a non-cohesive, dry medium grain sand with a mean grain diameter of d_{50}=0.8 mm. The hopper model was fixed at the bottom (it was supported by a steel rigid frame structure) (fig. 1). Twin plane, 12-electrode sensor was applied at different locations above the outlet; height values: h=[0.3m, 0.75m, 0.85m, 1m, 1.5m]. The vertical, axial length of the electrodes was equal to the diameter of the silo.

3. Packing density measurement

Before conducting the proper experiment it was checked measurement possibility of the changes of the small material concentration basing on the used ECT system. The tests were performed with a dry cohesionless sand with a mean grain diameter of d_{50}=0.8 mm. An initially loose sand was obtained by filling the silo from a small feeder hopper fixed above the silo (unit weight γ_{loose}=15.04 kN/m^3, 88.79kg in the silo volume). An initially dense sand (γ_{dense}=16.47 kN/m^3, 97.19kg in the silo volume) was obtained by filling the silo using a so-called "rain method" (through a vertically movable sieve located above the upper sand surface in the symmetry-axis). The knowledge about the different in the sand packing density can give the answer to question about the accuracy of the measurements.

Fig. 1. Experimental station photo.

The relationship between the packing density ratio of dense and loose sand can be calculated on the basis of the unit weight for two different types of the silo filling (eq.1):

$$r = \frac{\gamma_{loose}}{\gamma_{dense}} = 0.9132 \qquad (1)$$

The results of conducted experiment are presented on fig. 2. The presented measurement data are taken directly from records of the analogue-to-digital converter (ADC). The data show the level of voltage proportional to capacitance measurements. On the fig. 2 ADC data are calculated with the use of equation (eq.2):

$$\Delta ADC = ADC_{high} - ADC_{low} \qquad (2)$$

where ADC_{low} is the measurements for empty sensor, ADC_{high} is the measurements for sensor filled with sand.

The measurements were taken from two different position of sensor, located above the silo's outlet (h=0.3 m – represented at Fig. 2 as stars and for h=1.50m – with crosses). In comparison to the theoretical consideration the coefficient r can be represented in graphical form as the linear relationships between packing density (eq.3):

$$\gamma_{loose} = r * \gamma_{dense} \cdot \qquad (3)$$

On fig. 2 is shown the graphical comparison between the theoretical and ECT measurement value of packing density ratio. In Table 1 there are the value of calculated coefficient r based on ECT measurements.

The presented results show the possibility of measurement the small changes of concentration with average error 3.1% for lower sensor location and 1.7% for higher sensor location. The experiments were conducted for static object inside sensor. The next step included the measurement of the concentration changes during gravitational flow with constant velocity. These experiments could give answer how the small temporary changes of the concentration are reflected in the measurement capacitances.

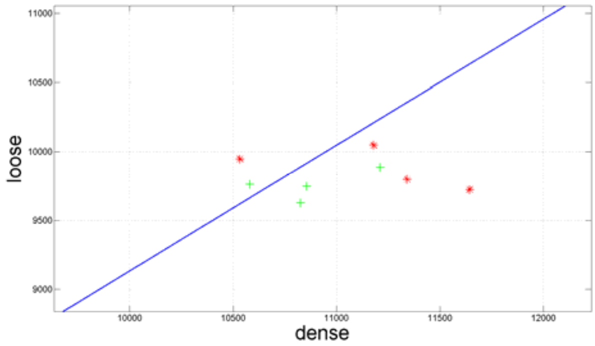

Fig. 2. Relation between different the initially packing density measurement in silo filled with sand (stars – h= 30m, crosses – h= 1.5m).

Table. 1. The calculated packing density ratio.

experiment nr:		1	2	3	4
h	0.3m	0.8639	0.8986	0.9442	0.8351
	1.5m	0.8978	0.9227	0.8819	0.8893

4. Flow monitoring

For the diagnosis point of view, especially, the sand behaviour along the silo wall (at various heights above the outlet) is very important due to the appearing dynamic effects, which can lead to vibrations, serious malfunction or even to construction catastrophe. The second localization in silo, which provides additional information about the silo discharge regularity is area of the funnel flow.

4.1. Capacitance raw measurements visualization for controlled discharging flow.

The designed laboratory setup allows to monitor the behaviour of the sand particles during constant outlet velocity v. The material was moving in whole the silo volume.

Fig. 3 presents graph of the normalized capacitance changes (C_{1-7} – the opposite electrodes) for sensor located at 1m and 0.3m above the outlet during controlled discharging process - velocity v=0.1mm/s. The similar character of the capacitance changes is visible for sensor located at 0.3 m above the outlet, these changes for lower material level are more noticeable. The results presented on fig. 3ab concern the filling the silo from a small feeder hopper. In case of the filling the silo with the use of the sieve the results are presented on fig. 3cd. The comparison of these capacitance changes (between dense and loose packing density) shows, that for the initially less packing density of sand, material is moving more dynamically.

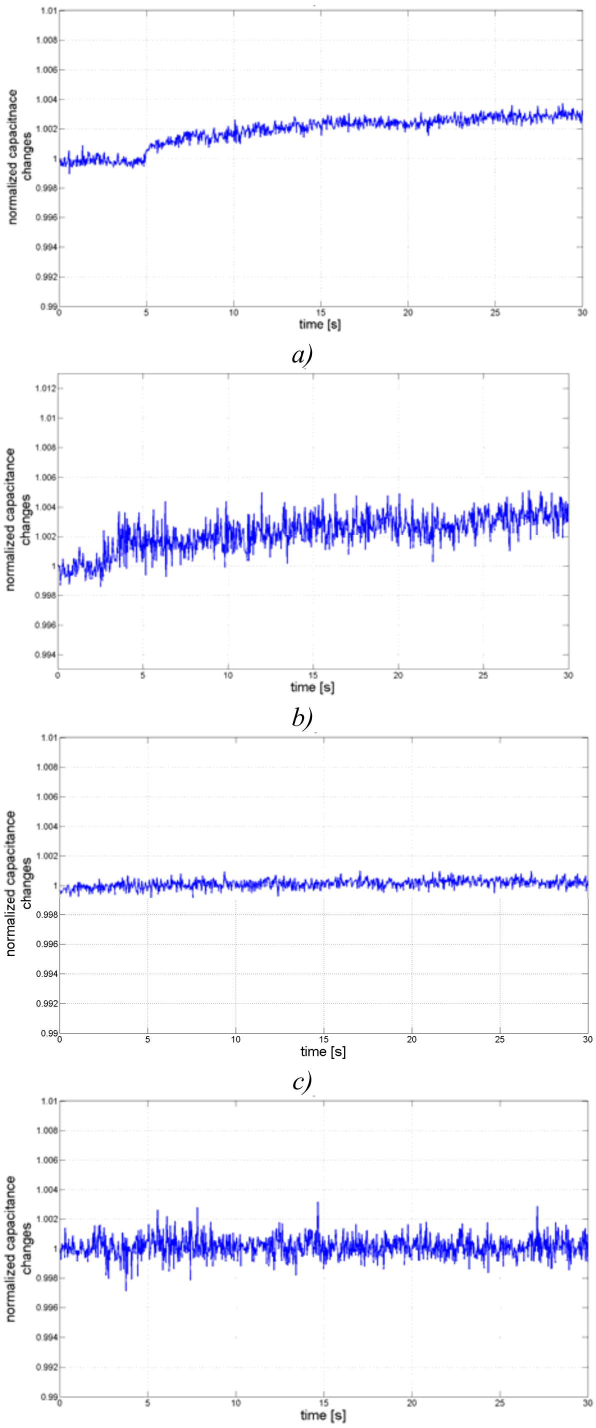

Fig. 3. Normalized capacitance changes (the opposite electrodes) in funnel area for sensor located at 1m and 0.3m above the outlet with controlled discharging - velocity v=0.1mm/s: a) loose sand, measured on 1.0 m; b) loose sand, measured on 0.3 m; c) dense sand, measured on 1.0 m; d) dense sand, measured on 0.3 m.

In order to measure the sand concentration near the silo wall, the adjacent electrodes capacitance values are the simplest and effective indicator to monitor phenomena appearing at wall comparing to tomography images interpretation.

Fig. 4 reveals the capacitance changes caused by sand behaviour near to the silo wall. Comparing these two examples (for initial dense and loose packing) the significant difference in sand particle behaviour is visible. For the loose packing of sand the concentration is increasing, the changes are very small, what is reason of very small changes of packing density. In the case of dense packing the change character of capacitances is dissimilar, the sand concentrations is decreasing.

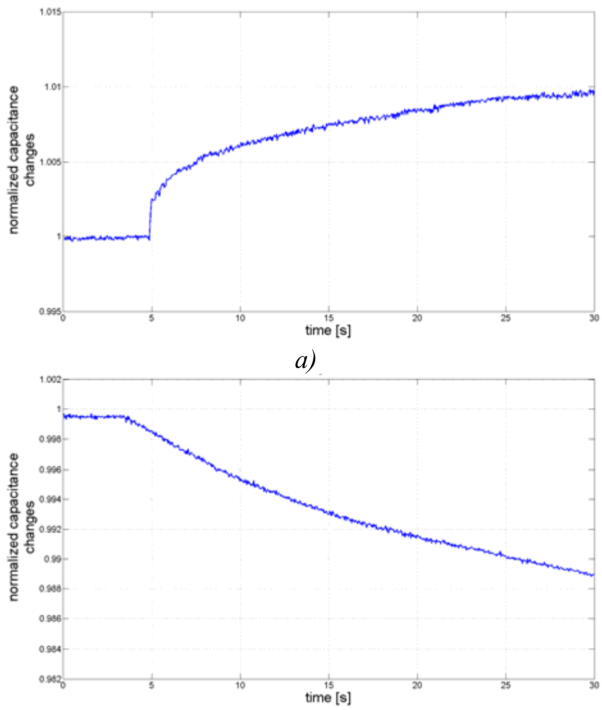

Fig. 4. Normalized capacitance changes (the adjacent electrodes) in stagnant zone, for sensor located at 1m above the outlet with controlled discharging - velocity v=0.1mm/s: a) loose sand; b) dense sand

Another conclusion arising from the conducted experiments concerns the noise level in the measurement. It is very important for corrected interpretation small changes of material concentration during silo discharge process based on the measurements. The noise can be specify by analysis of the first fragment of the graph, when silo outlet was still closed. The corresponding noise for the distinct plots of Fig. 3-4 is at range of about $1.2 \div 0.4 * 10^{-3}$.

The changes in the measured capacitances are reflected in reconstructed tomography images. The sequence of tomography images in form of topograms are shown at fig. 5. On the X-axis is the time scale, on the Y-axis are the pixels number constitute the cut-off line of the sensor cross-section. Such presented tomography data allows easily visualization of the significant difference in the sand behavior during the flow. The concentration in case of the silo filling from a small feeder hopper – loose packing – (fig. 5a) is decreased in the silo centre and is increased close to the silo wall. The situation is opposite to the one initially dense packed sand (fig5b). In this case the sand concentration close to the silo wall is smaller than in the silo centre. The concentration at the silo wall is almost constant during flow. The other important difference between these two cases concerns the time delay between the time of the outlet opened and the capture time of the concentration changes at sensor level. For the initially dense packed material, the time delay is bigger.

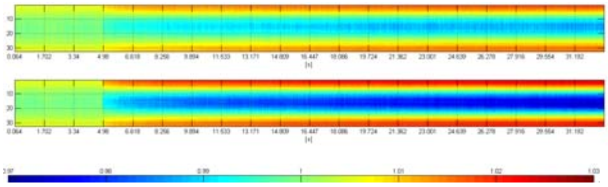

a)

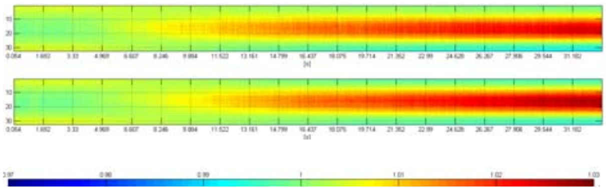

b)

Fig. 5. Topograms - the sequence of vertical cross of tomography images in time, controlled velocity of discharging 0.1 mm/s, measurement on h=1.0m: a) smooth wall, loose sand; b) smooth wall, dense sand

4.2. Gravitational discharging flow imaging

One of the mayor aims of presented work was the monitoring of dynamic effects appearing during the silo discharging process. The interaction between the material and silo structure effects as an acoustic signal caused by pronounced pulsations of the solid concentrated in the upper part of the silo due to dynamic effects and the vibration of silo construction during the unloading process. Concentration changes for different position of pixels – pixel at the silo wall p(1,15) and pixel in the silo centre p(15,15) at location of sensor are presented at the fig. 6÷10. The measurements were conducted at 5 different height above the outlet h=[0.3m, 0.75m, 0.85m, 1.00m, 1.50m]. The fig. 6 shows the concentration changes for h=0.3m and h=1.5m above the outlet. For higher sensor location characteristic oscillation appeared, which is the effect of the mentioned the resonance between silo and sand. For h=0.3m the oscillations are smaller (and for the centre pixel no oscillations are present). The topogram, presented on fig. 7a, depicts the concentration changes in the whole length of sensor cross-section. In order to illustrate the oscillations, fig. 7b presents the magnified segment for h=1.5m.

Fig. 8-9 present dynamics effects in form of the oscillations appearing during flow – for sensor located at around the half of the silo height. This particular silo height value is very interesting for analysis of the phenomena of flow regime changes (mass flow and funnel flow). Fig. 8 reveals the comparison of the concentration characteristic plots for h=0.75m and h=0.85m.

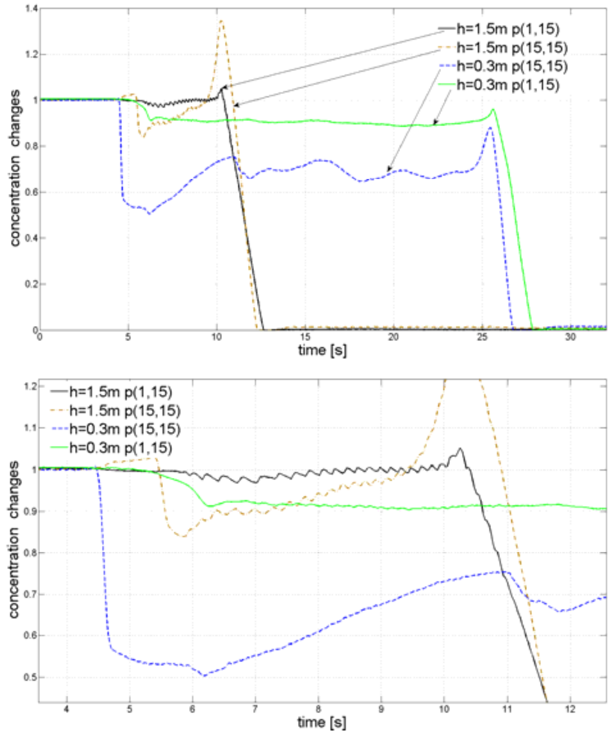

Fig. 6. Concentration changes during the silo discharging for initially dense packing sand with the smooth silo wall, height of sensor position and analysed point selection like on legends.

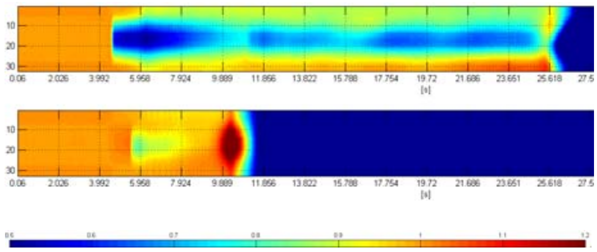

a)

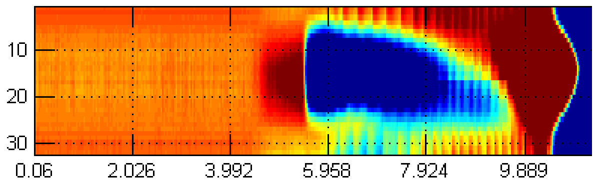

b)

Fig. 7. Topograms - concentration changes in the whole length of sensor cross-section, b) h=0.3m and h=1.5m, b) magnification emphasizes the oscillations for h=1.5m in fig. 6

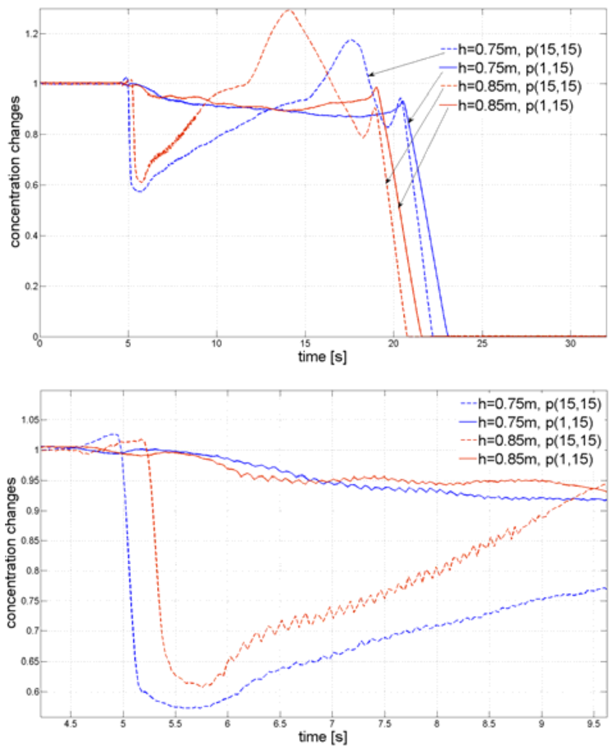

Fig. 8. The concentration changes during the silo discharging for initially dense packing with the smooth silo wall, dense sand, height of sensor position (h=0.75m and 0.85m) and analysing point selection (centre or close to the wall) like on legends.

For the above mentioned silo heights, the oscillations are visible for each location inside the sensor space, but especially evident for h=0.85m. Fig. 9 reveals the comparison of the concentration changes for h=0.85m and h=1m.

The presented results show that the biggest oscillations appearing at 0.85m above the outlet, what can be result of the flow regime change (form mass flow to the funnel flow). Oscillations disappear in the lower part of the silo when funnel flow takes place (fig. 6 h=0.3m). The monitoring of these dangerous oscillations is very important; this phenomenon can be minimized by application of the rough silo wall. Fig. 10 presents results for sensor located at h=0.3m and h=1.5m above the outlet with irregular wall surface. Sandpaper was stuck to the silo wall.

The rough wall is also crucial to the concentration distribution for the lower sensor location (h=0.85m). The presence of sandpaper causes the decrease of packing density at wall area – in the time interval 10…19 seconds on fig. 10 the wall shear zone is visible.

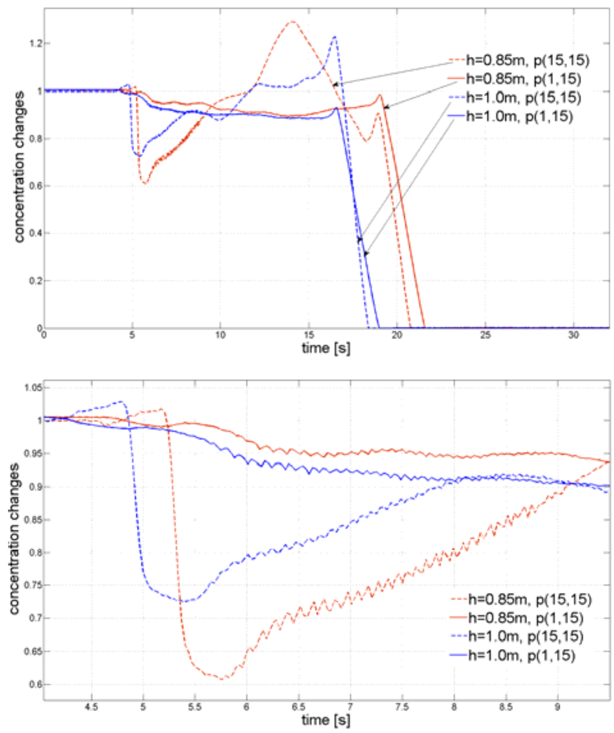

Fig. 9. The concentration changes during the silo discharging for initially dense packing with the smooth silo wall, dense sand, height of sensor position (h=0.85m and 1.0m) and analysing point selection (centre or close to the wall) like on legends.

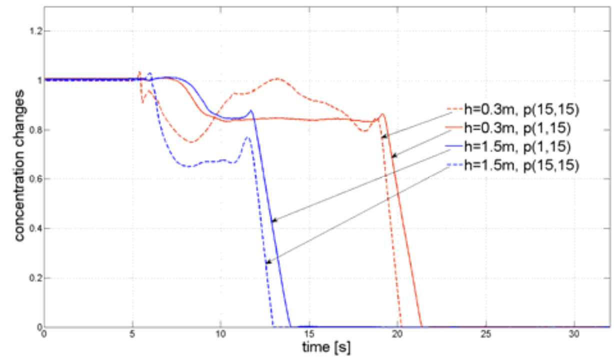

Fig. 10. The concentration changes during the silo discharging for initially dense packing with the rough silo wall, dense sand, height of sensor position (h=0.3m and 1.5m) and analysing point selection (centre or close to the wall) like on legends.

5. Remarks and conclusions

The paper covers the way of formulating the description for the hopper discharging dynamics. Accurate monitoring of the silo discharging can lead to proper control of this process. In order to achieve this aim, two possibilities of tomography data processing methods were analysed. First, raw capacitance measurements were considered, and then, tomography imaging was evaluated.

The capacitance measurement is in fact an indicator of dielectric permittivity coefficient associated with an investigated material in the measurement space. The material distribution inside a measurement space is described by the associated dielectric permittivity, which has a direct influence on the measured values of capacitance. The dielectric permittivity distribution is proportional to the material concentration (Pląskowski et al., 1995; Jaworski and Dyakowski, 2002).

The first part of the presented results – static tests and flow control experiments – showed direct relationship of the capacitance measured values to the real values of the porosity of the bulk solid. Moreover, the possibility of accurate estimation of the material packing density based on ECT system application was proved. Such ECT-originated results analysis feasibility is very important, specially for industrial processes, when expected changes in material concentration are at the 10% variation level. Analysis and interpretation of the capacitance changes in function of time confirms the practical ECT application for the purposes of monitoring and control of the silo discharging process.

The second part of the demonstrated results proved the possibility to measure the oscillations during the silo discharging process. Moreover, investigation of the wall roughness and initial packing density level influence on the dynamics effects scale was conducted, as well. The experiments were conducted for different configuration of the measurement setup. Measurement records were taken at various heights above the silo outlet, which allowed to analyse both: mass flow (at the higher position of sensor) and funnel flow (for the low position of sensor).

Acknowledgements

The authors thank the Polish Committee of Science Research (167/6, PR UE/2007/7).

REFERENCE

BATES L., (1999), Problems In Particulate Flow, Part A -- Flow Regimes, Ajax Equipment Ltd. Mule Street, United Kingdom, http://www.erpt.org/992q/Bate-00.Htm.

CHANIECKI Z., SANKOWSKI D., (2007), Monitoring and diagnosis of dynamics states using process tomography (in polish), Diagnostics of processes and systems, DPS 2007, EXIT, ISBN 978-83-60434-31-4, pp. 387-394, 456pp.

CHANIECKI Z. (2006), Algorithms of data processing and analysis in electrical capacitance tomography for diagnosis of selected industrial processes. PhD thesis (in Polish). Technical University of Łódź, Łódź, pp.1-258.

CHANIECKI Z., DYAKOWSKI T., NIEDOSTATKIEWICZ M., SANKOWSKI D. (2006), Application of electrical capacitance tomography for bulk solids flow analysis in silos. Particle and Particle Systems Characterization, 23, 3-4, pp.306-312.

CHANIECKI Z., NIEDOSTATKIEWICZ M., DYAKOWSKI T., PLĄSKOWSKI A., SANKOWSKI D., SMOLIK W., SZABATIN R., (2004), Badania dynamiki przepływu w silosach-informacja o wstępnych pracach nad wprowadzeniem pojemnościowej tomografii procesowej, (in polish) W: Byrski W., Mikrut Z. (red.), Automatyka, UWN-D, Kraków, 8 (3), pp. 381-390.

CHASE G.G., (2002), Solids Notes 10 - Hopper Design, The University of Akron, The Department of Chemical Engineering, http://www.ecgf.uakron.edu/~chem/fclty/chase.

DYAKOWSKI T., WANG S.J., XIE C.G., WILLIAMS R.A., BECK M.S., (1993), Real time capacitance imaging of bubble formation at the distributor of a fluidised bed, Chemical Engineering Journal, Vol.56, pp.95 -100.

GRUDZIEN K., ROMANOWSKI A., AYKROYD R.G., WILLIAMS R.A., WEST R.M., MENG S., (2004), Application of the Bayesian Approach to Powder Flow Investigation, 3rd International Symposium on Process Tomography in Poland, Lodz, p. 72-76.

GRUDZIEŃ, (2007) The Segmentation Algorithms for Diagnosis Parameters Visualization of Multiphase Flows in Chosen Industrial Systems, PhD thesis, (in polish), Technical University of Lodz, pp.1-199.

JAWORSKI A.J., DYAKOWSKI T., (2002), Investigations of flow instabilities within the dense pneumatic conveying system, Powder Technology, 125, 2-3, pp. 279-291.

JENIKE A.W., (1970), Storage and Flow of Solids, Engg. Exp. Station Bulletin, 123 (University of Utah).

KORBICZ J., KOŚCIELNY J.M., KOWALCZUK Z., CHOLEWA W. (ed.), (2002), Diagnostyka procesów. Modele. Metody sztucznej inteligencji. Zastosowania, (in polish), WNT, 828 pp.

LIONHEART B., (2001), Reconstruction Algorithms for Permittivity and Conductivity Imaging, 2nd World Congress on Industrial Tomography, Hanover 2001, pp.4-11.

NEUFFER D., ALVAREZ A., OWENS D.H., OSTROWSKI K.L., LUKE S.P., WILLIAMS R.A., (1999), Control of Pneumatic Conveying Using ECT, 1st World Congress on Industrial Process Tomography, pp. 71-76.

NIEDOSTATKIEWICZ M., TEJCHMAN J., (2003), Experimental and theoretical studies on resonance dynamic effects during silo flow. Powder Handling & Processing, 15, 1, 36-42, 2003.

OSTROWSKI K., LUKE S.P., BENNETT M.A., WILLIAMS R.A., (1999), Application of capacitance electrical tomography for on-line and off-line analysis of flow pattern in horizontal pipeline of pneumatic conveyor, Chemical Engineering Journal, 3524, pp.1-8.

PLĄSKOWSKI A., BECK M.S., THORN R., DYAKOWSKI T., (1995), Imaging Industrial Flows: Applications of Electrical Process Tomography, IOP Publishing, Bristol, p.232.

ROMANOWSKI A., GRUDZIEN K., WILLIAMS R.A., (2006), Analysis and Interpretation of Hopper Flow Behaviour Using Electrical Capacitance Tomography, Particle & Particle Systems Characterization, Volume 23, Issue 3-4, p. 297-305

SEVILLE JPK., TUZUN U., CLIFT R., (1997), Processing of Particulate Solids, Blackie Academic, London, p. 377.